JOURNAL OF SOLID STATE CHEMISTRY 9, 336–344 (1974)

The Kinetics of Silica Reduction in Hydrogen*

RICHARD A. GARDNER

IBM System Products Division, East Fishkill Laboratory, Hopewell Junction, New York 12533

Received July 2, 1973

The kinetics of the reduction of SiO_2 in hydrogen have been examined using a thermalgravimetric method. The mechanism of the reaction $SiO_2 + H_2 = SiO + H_2O$ can be described on the basis of a reaction interface moving at a constant velocity toward the center of the reacting sample. The velocity of the moving interface depends on the reaction temperature and water vapor content of the ambient gas. The reaction was studied in the temperature range 1115–1630°C and was found to be isokinetic in this range. The activation energy for the reaction is 85 kcal/mole in pure, dry hydrogen and 135 kcal/mole in hydrogen with a dew point of 24°C.

Introduction

The reaction of silicon dioxide with gaseous hydrogen to form volatile silicon monoxide and water vapor is important in many high-temperature ceramic and metallurgical applications. The reduction of SiO_2 has been extensively studied by a number of investigators (*1–6*), with the primary interest being the equilibrium thermodynamics of the reaction. Toropov and Bakzokovskii (*7*) reviewed the literature concerning oxidation–reduction equilibria involving silicon monoxide up to about 1963 and pointed out many discrepancies concerning the equilibria. The kinetics of the reduction of silica, however, have received little attention. Schwerdtfeger (*8*) and Crowley (*9*) studied the rate of silica loss in reducing atmospheres by weighing fused quartz spheres and silica-containing samples, respectively, before and after heat treatments and concluded that the rate of silica reduction in hydrogen is controlled by convective diffusion or mass transfer from the reacting surface. This conclusion was based on the dependence of the rate of weight loss on hydrogen flow rates. Although Schwerdtfeger's data fit the general form of the rate equations for convective diffusion, the reduction rates were lower than those predicted by a factor of about 2. Schwerdtfeger noted the discrepancy and indicated that it may have been due to a contribution of a slow surface reaction. The rate of silica reduction in carbon monoxide–carbon dioxide mixtures, however, was not affected by gas flow rates, and Schwerdtfeger concluded that in this case the rate is controlled by a slow surface reaction. In a thermodynamic study of silicon monoxide, Ramstad and Richardson (*5*) found a dependence of the partial pressure of SiO on hydrogen flow rates at low flow rates (less than about 75 ml/min) but found no dependence at higher flows.

Because the loss of silica can cause considerable changes in the properties of high-temperature ceramic materials, a study was undertaken to more thoroughly document the kinetics of the reduction of silica by hydrogen.

Experimental

A schematic diagram of the experimental apparatus is shown in Fig. 1. The furnace is a water jacket-cooled, graphite-element furnace. The furnace is capable of achieving temperatures of over 2000°C, but the use of hydrogen gas required incorporation of a high-purity aluminum oxide muffle; this limited the useful temperature range up to approximately 1700°C. The internal diameter of the muffle was 4.60 cm. The maximum temperature used was 1630°C. Argon and hydro-

* Portions of this paper were presented at the American Ceramic Society 75th Annual Meeting, April 29–May 3, 1973, Cincinnati, Ohio.

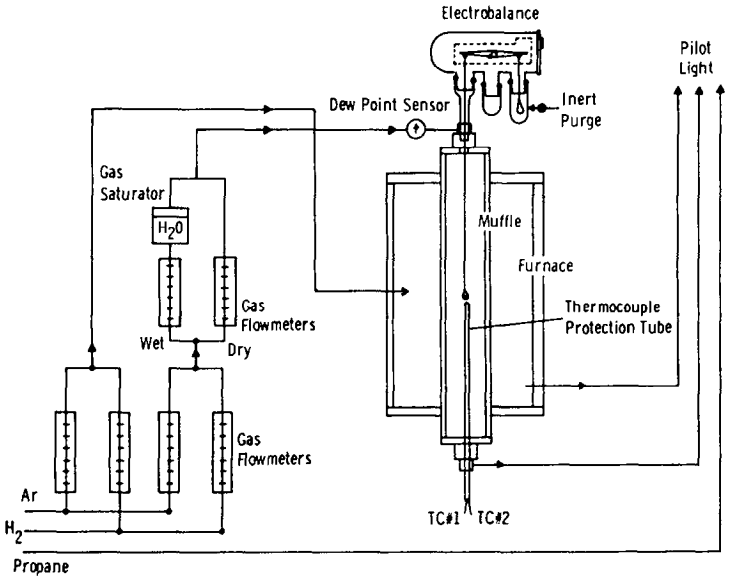

FIG. 1. Schematic diagram of experimental apparatus.

gen were delivered to the furnace as shown. The gases were approximately 99.999% pure with 2 ppm water. The moisture content was determined with a Beckman Trace Moisture Analyzer. The diagram shows that a gas saturator was built into the system to permit addition of water vapor to the reaction gas. The dew point of the gas delivered to the reaction chamber was monitored by means of a dew point hygrometer. The flow rate of the gas was maintained at 4 ft^3/hr. All exit gases were burned off using a propane pilot light for safety reasons.

The weight of the sample was monitored using a Model RG electrobalance from the Cahn Division of Ventron. The sample was suspended from the balance using a 0.008-in. molybdenum wire and contained in a molybdenum basket fabricated from 0.001-in. foil. The molybdenum was 99.99% pure.

The temperature of the furnace was controlled using a solid-state proportional band controller in conjunction with a curve-following temperature programmer. The controller was able to maintain the temperature constant during the isothermal experiments to within ±5°C. Two grounded Pt 6% Rh–Pt 30% Rh thermocouples were used for temperature measurement. One thermocouple was attached to the temperature controller and the other to one channel of a dual-channel multirange potentiometric strip-chart recorder. The other channel of the recorder was used to continuously monitor the weight of the reacting sample.

The electrobalance was mounted on an electrical hoist so that the balance with the attached hangdown wire and sample basket could be lowered into place. The balance was calibrated before each run with the sample basket and hangdown wire attached. The system was purged with hydrogen for a minimum of 30 min before each experiment. During the heating portion of the cycle, which required approximately 40 min, the gas was passed through a water bubbler at room temperature in order to saturate the reaction gas. This was done to retard the silica reduction before the isothermal reaction temperature was reached. During the heating portion of the cycle, the extent of the reaction was only on the order of 0.01–0.03% or less depending on the reaction temperature. Dry (nonsaturated) hydrogen was admitted to the reaction chamber when the furnace reached the isothermal reaction temperature, and this point was taken as zero time. For reactions in hydrogen saturated with water vapor, zero time was taken as the time at which the furnace reached the isothermal reaction temperature.

Three forms of silica were used as samples in this study: clear fused quartz rod and tubing samples with purities of 99.9% from the General Electric Co. and high-purity quartz powder from Engineering Materials, Inc. The diameter of the

rod was 0.203 cm, and the dimensions of the tubing were 0.396 cm o.d. and 0.284 cm i.d. Most of the experiments were carried out with tubing samples to eliminate the effects of surface area changes during a kinetic run since decreases in the outer surface area are compensated for by increases in the inner surface area. The rod and tubing samples were generally 0.84 cm in length, and the samples had surface areas of 0.6 and 1.8 cm^2, respectively. The surface area of the quartz powder was measured using the standard B.E.T. gas adsorption technique with krypton as an adsorbate and was found to be 1.3 m^2/g. Powder sample sizes were approximately 100 mg.

Treatment of Data

Hancock and Sharp (*10*) have described a convenient method of comparing the kinetics of isothermal solid-state reactions based on an equation describing nucleation and growth processes. The equation

$$\alpha = 1 - \exp(-\beta t^m) \qquad (1)$$

or

$$-\ln\ln(1-\alpha) = \ln\beta + m\ln t$$

was derived by Johnson and Mehl (*11*) and by Avrami (*12*) and proposed by Erofe'ev (*13*) for a generalized equation for solid-state reaction kinetics. In the above equation, α is the fraction reacted at time t, β is a constant which partially depends on nucleation frequency and rate of grain growth, and m is a constant that varies with the geometry of the system. Hancock and Sharp pointed out that kinetic data which follow any one of a number of kinetic equations, including the equations for nucleation and growth processes, give rise to approximately linear plots of $-\ln\ln(1-\alpha)$ vs $\ln t$ if the range of α is limited to values 0.15–0.50. The slopes of such plots are diagnostic of the reaction mechanism.

Hancock and Sharp treated nine kinetic equations which could arbitrarily be separated into three groups; these represented (a) diffusion-controlled reactions, (b) phase-boundary-controlled and first-order reactions, and (c) reactions which obey the Avrami–Erofe'ev equations. The group to which a reaction belongs can readily be established by noting the slopes of plots of $-\ln\ln(1-\alpha)$ vs $\ln t$. Table I presents the equations considered. The functions $D_1(\alpha)$ through $D_4(\alpha)$ represent some of the important diffusion equations. $F_1(\alpha)$ is the function for first-order reactions, and $R_2(\alpha)$ and $R_3(\alpha)$ are the equations for phase-boundary-controlled reactions for a cylinder (or circular disc) and a sphere, respectively. $A_2(\alpha)$ and $A_3(\alpha)$ are the Avrami–Erofe'ev equations for $m = 2.00$ and 3.00, respectively. It can be seen that values for m range from 0.54 to 0.62 for diffusion-controlled reactions, 1.00 to 1.11 for first-order and phase-boundary controlled reactions, and 2.00 and 3.00 for the Avrami–Erofe'ev equations.

TABLE I

SOLID-STATE REACTION RATE EQUATIONS

Function	Equation	m^a
$D_1(\alpha)$	$\alpha^2 = kt$	0.62
$D_2(\alpha)$	$(1-\alpha)\ln(1-\alpha)+\alpha = kt$	0.57
$D_3(\alpha)$	$[1-(1-\alpha)^{1/3}]^2 = kt$	0.54
$D_4(\alpha)$	$1-2\alpha/3-(1-\alpha)^{2/3} = kt$	0.57
$F^1(\alpha)$	$-\ln(1-\alpha) = kt$	1.00
$R_2(\alpha)$	$1-(1-\alpha)^{1/2} = kt$	1.11
$R_3(\alpha)$	$1-(1-\alpha)^{1/3} = kt$	1.07
Zero order	$\alpha = kt$	1.24
$A_2(\alpha)$	$[-\ln(1-\alpha)]^{1/2} = kt$	2.00
$A_3(\alpha)$	$[-\ln(1-\alpha)]^{1/3} = kt$	3.00

[a] $-\ln\ln(1-\alpha) = \ln\beta + m\ln t$.

The phase-boundary-controlled and first-order equations are of particular importance in this study. If a cylinder or circular disc reacts from the edge inward and the reaction is controlled by the movement of an interface at a constant velocity μ, then α and t can be related by the function $R_2(\alpha)$. The rate constant k in this equation is equal to μ/r, where r is the radius of the sample. Similarly, for a sphere reacting from the surface inward, the fraction reacted and time are related by the function $R_3(\alpha)$. Plots of $R_2(\alpha)$ or $R_3(\alpha)$ vs t will be linear if the reaction is controlled by one of these mechanisms.

The fraction reacted, α, was calculated in this study by monitoring the weight of the silica sample on a strip chart running at a known speed and comparing the weight at time t to the initial weight.

Results and Discussion

Plots of $-\ln\ln(1-\alpha)$ vs $\ln t$ for quartz samples reacted in dry hydrogen are shown in Fig. 2. These plots all have slopes of 1.05 ± 0.8, indicating that the reaction within this temperature

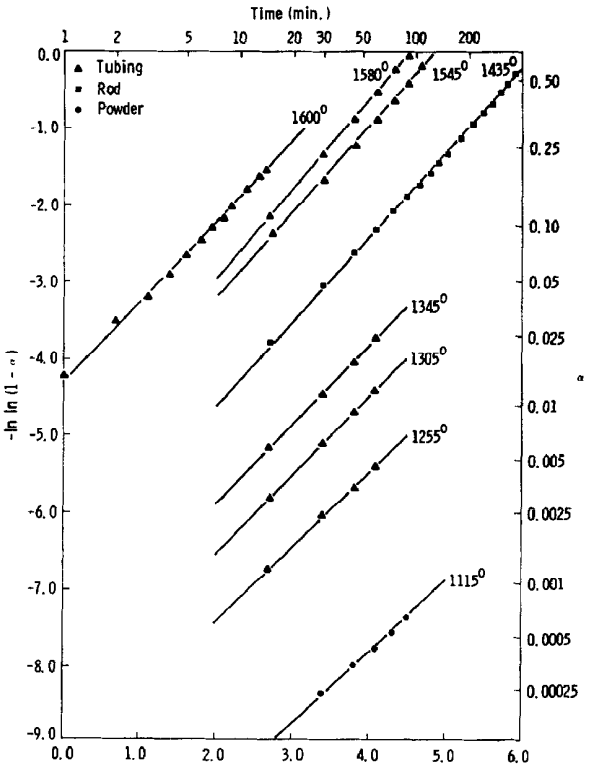

FIG. 2. Plots of $-\ln\ln(1-\alpha)$ vs $\ln t$ for reduction of quartz samples in dry hydrogen.

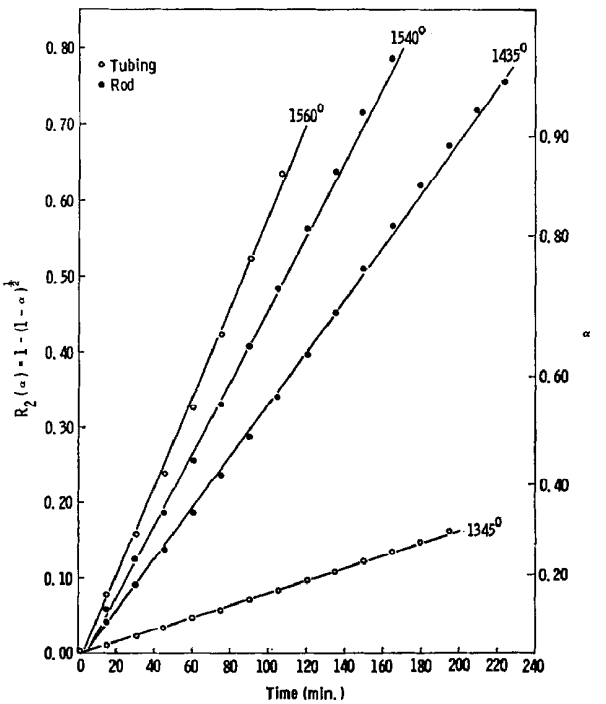

FIG. 3. $R_2(\alpha)$ versus time for quartz tubing and rod samples reacted in dry hydrogen.

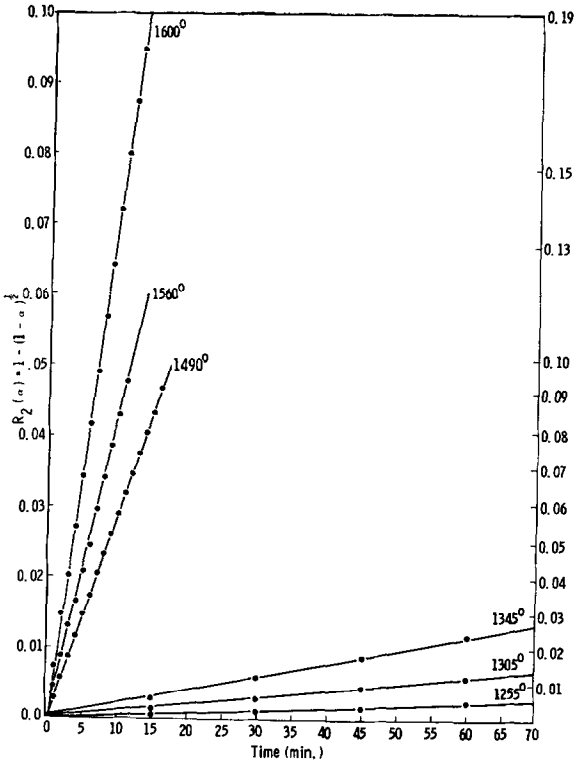

FIG. 4. $R_2(\alpha)$ versus time for quartz tubing reacted in dry hydrogen. All plots are for the same sample.

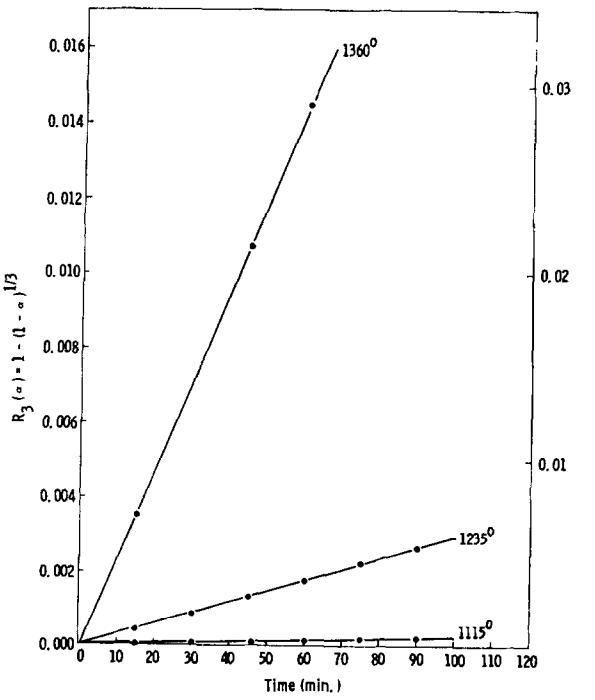

FIG. 5. $R_3(\alpha)$ versus time for quartz powder reacted in dry hydrogen.

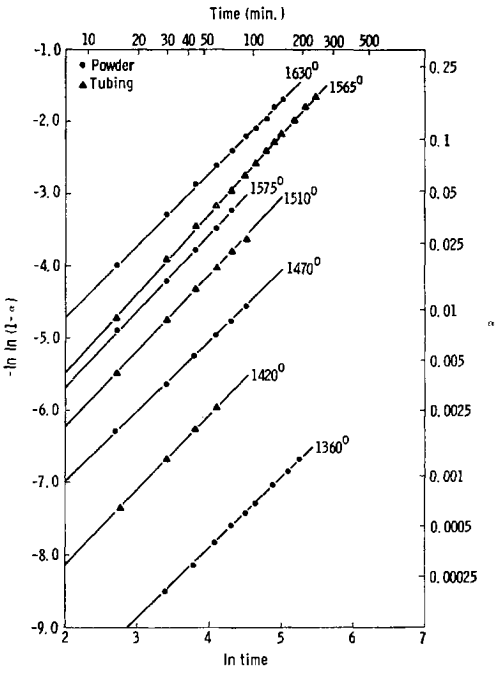

FIG. 6. Plots of $-\ln\ln(1-\alpha)$ vs $\ln t$ for reduction of quartz samples in wet hydrogen (dew point = 24°C).

range is isokinetic, i.e., the mechanism is the same at all the temperatures studied. The slope of the plots suggests that the reaction can be described using equations deduced on the basis of a reaction interface contracting inwards from the surface of a cylinder or sphere, depending on the geometry of the sample. Plots of $R_2(\alpha)$ or $R_3(\alpha)$ versus time should therefore be linear.

Figure 3 presents isothermal kinetic plots of $R_2(\alpha)$ versus time for rod and tubing samples. As predicted, the graphs are linear, indicating excellent agreement with the theoretical equation. Data for Fig. 3 are for experiments in which the reaction was allowed to run to greater than 90% completion for the reactions above 1400°C. Figure 4 presents data for the reaction of quartz tubing for which the temperature was not held constant for the complete reaction. Instead, several kinetic runs were made for the same sample by changing the temperature several times during the experiment and holding a particular temperature until enough data was obtained to permit accurate calculation of the rate. No acceleration period was noted in that as soon as the temperature became isothermal, the rate of weight loss became essentially linear.

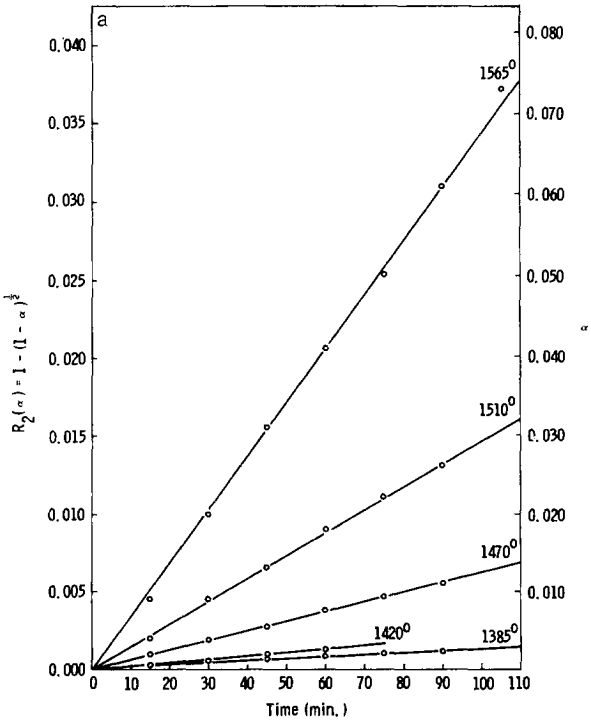

FIG. 7a. $R_2(\alpha)$ versus time for quartz tubing reacted in wet hydrogen (dew point = 24°C).

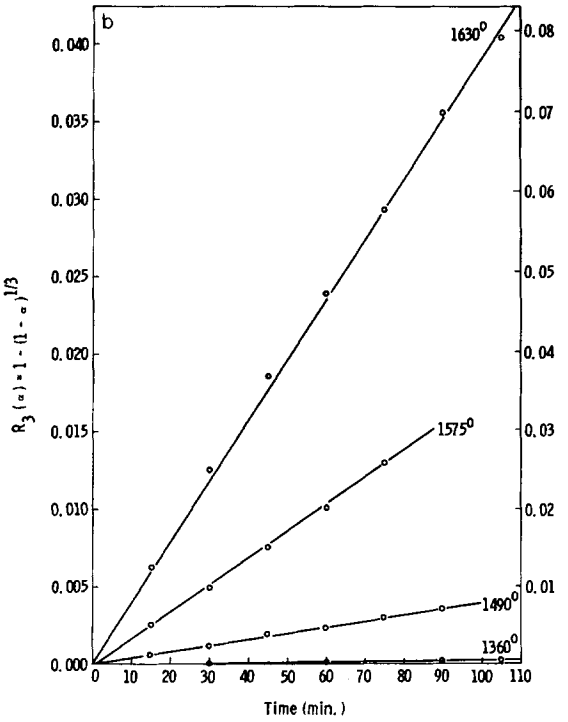

FIG. 7b. $R_3(\alpha)$ versus time for quartz powder reacted in wet hydrogen (dew point = 24°C).

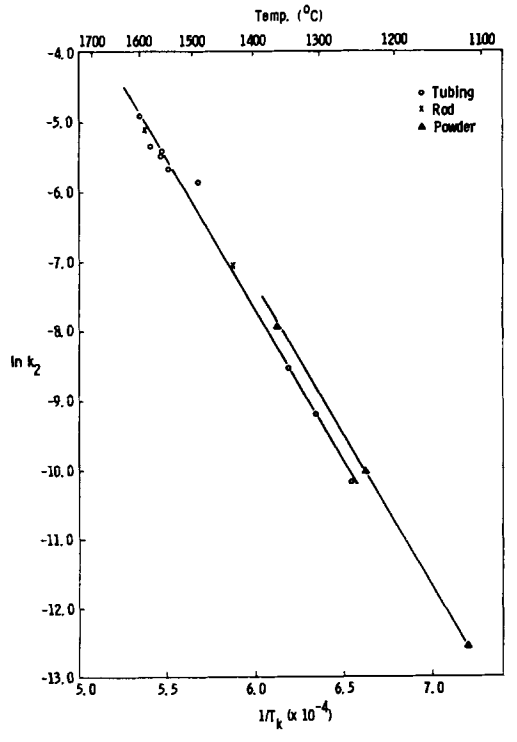

FIG. 8. Arrhenius diagram for calculation of activation energy. Samples reacted in dry hydrogen.

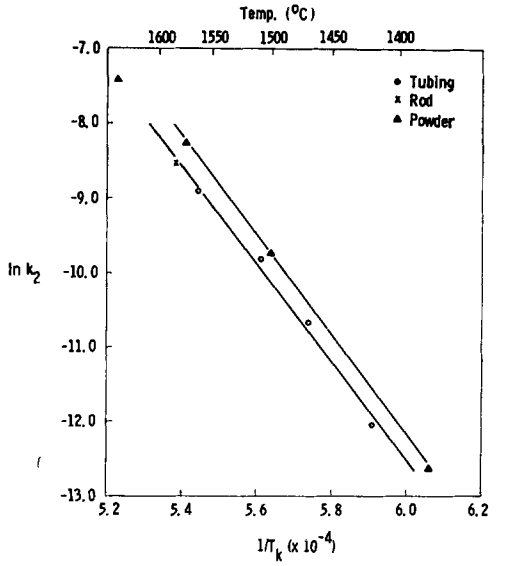

FIG. 9. Arrhenius diagram for calculation of activation energy. Samples reacted in water-saturated hydrogen.

Plots of $R_3(\alpha)$ versus time for powder samples are shown in Fig. 5. As before, the plots are linear. The lowest temperature at which a measurable rate was obtained was 1115°C. It is likely that the rate could be measured at still lower temperatures by extending the times for data collection. Crowley (*9*) reports a minimum reaction temperature of about 925°C.

Silica samples reacted in wet hydrogen with a dew point of 24°C behaved similar to samples reacted in the pure hydrogen. Figure 6 shows $-\ln\ln(1-\alpha)$ vs $\ln t$ for samples reacted in the water-saturated hydrogen. In this case, the average slope is $1.03 \pm .06$. As in the case of the reaction with dry hydrogen, the reaction can be described using equations for phase-boundary-controlled reactions. Figures 7a and 7b present plots of $R_2(\alpha)$ and $R_3(\alpha)$ for silica samples reacted in wet hydrogen. The linearity of the plots indicates good agreement with the theoretical equations.

Arrhenius plots of the reaction rates in dry hydrogen are shown in Fig. 8. The linearity of the graphs for the rod and tubing samples indicates that the differences in the surface areas of these samples are not significant. The rates of reaction for the powdered samples, however, are slightly higher than the corresponding rates for the cylindrical samples. This is as expected. The activation energy for the reaction in dry hydrogen is 85 kcal/mole. Figure 8 shows no change in the

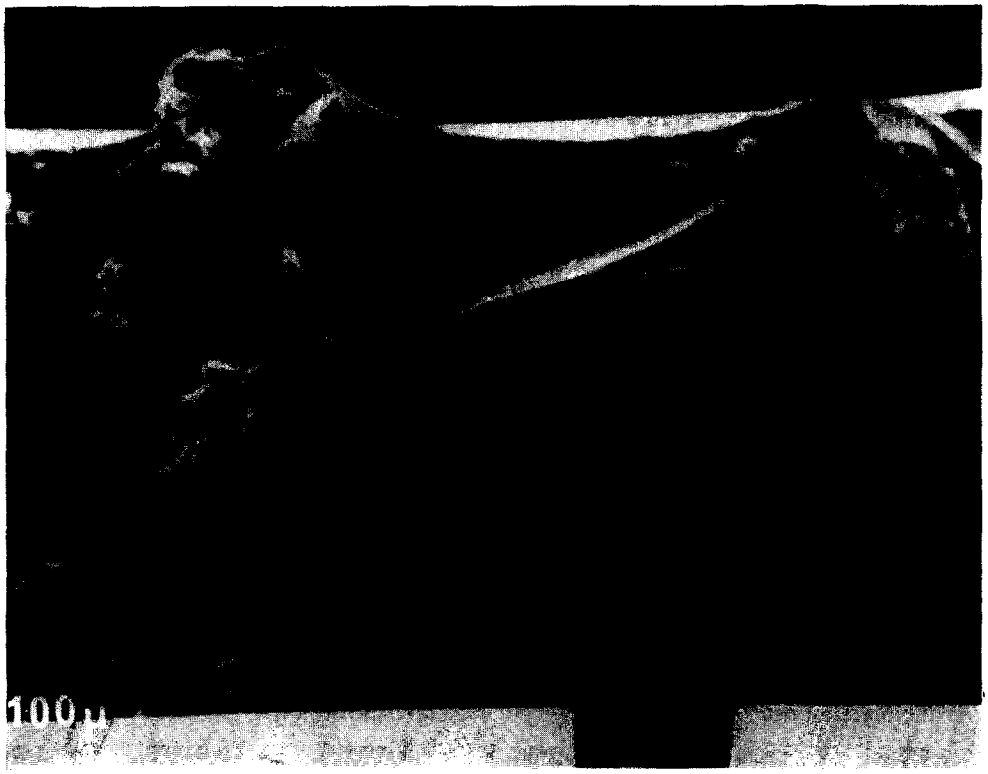

FIG. 10a. Surface and interface of fused quartz rod reacted in hydrogen. Original magnification: 200×.

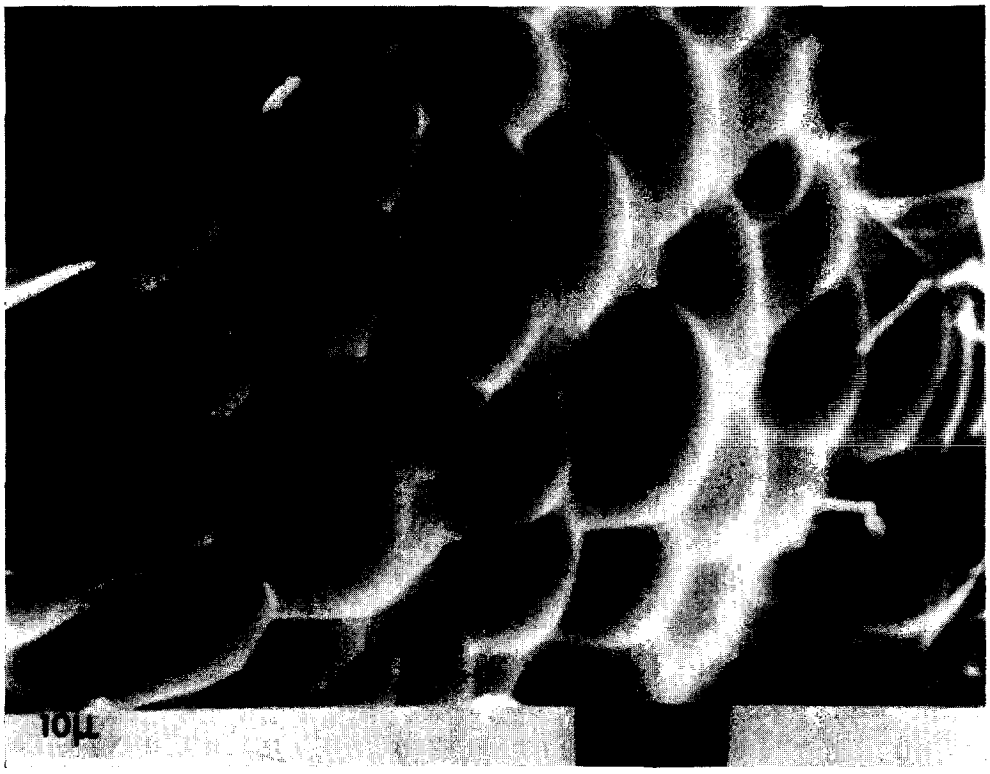

FIG. 10b. Surface of fused quartz rod reacted in hydrogen. Original magnification: 2000×.

activation energy above and below the cristobalite transition temperature of 1470°C.

Figure 9 is an Arrhenius plot for samples reacted in wet hydrogen (dew point = 24°C). In this case, the activation energy is 135 kcal/mole. The figure indicates that, as in dry hydrogen, the rate of reaction is greater for the powdered quartz samples than for the cylindrical samples.

Visual observation of samples removed from the furnace before the reaction was completed indicated that the surface appeared to be recrystallized. X-ray diffraction of the reacted sample showed the presence of α-cristobalite. Examination of the sample using electron microscopy revealed the interesting surface topography shown in Figs. 10a and 10b. The surface is covered with dome-shaped "grains." This indicates a preferential attack of the hydrogen at the grain boundaries.

It was found that the flow rate of the gas did not affect the rate of reaction in the range of flow rates studied. Changes in the hydrogen flow rate from 2 to 10 ft^3/hr produced no observable change in the reaction rate.

Conclusion

A possible reaction sequence for the reduction of silica by hydrogen can be postulated as follows: (a) adsorption of hydrogen on the silica surface to form an active site; (b) surface reaction of silica and adsorbed hydrogen to form silicon monoxide and water; (c) desorption of SiO and H_2O; (d) convection or transport of the reaction products away from the reaction surface. The overall rate is controlled by the slowest of these steps. The works of Schwerdtfeger and of Crowley indicated that the mass-transport step is rate determining due to the dependence of the reaction rate on atmosphere flow rates. No such dependence, however, was found in this study within the range of flows examined. Instead, the rate was found to closely obey kinetic equations for the movement of a reacting interface. This indicates that a slow surface reaction is rate controlling.

The fact that the activation energy varies from 85 kcal/mole for reaction in dry hydrogen to 135 kcal/mole for reaction in water-saturated hydrogen indicates a change in the mechanism of the reaction. This change probably results from the formation of Si–OH groups on the surface of the sample which effectively lowers the surface activity of the silica. Fewer sites are then available for the adsorption of hydrogen and the rate of reaction is lowered.

Acknowledgment

The author acknowledges the efforts of William R. Swiss in helping to set up and optimize the experimental apparatus. Discussions with Dr. Relva C. Buchanan were also helpful.

References

1. G. Grube and H. Speidel, *Z. Elektrochem.* **53**, 339 (1949).
2. H. Schafer and R. Hornle, *Z. Anorg. Allg. Chem.* **263**, 261 (1950).
3. N. C. Tombs and A. J. E. Welch, *J. Iron Steel Inst. London* **172**, 69 (1952).
4. K. G. Gunther, *Glastech. Ber.* **31(1)**, 15 (1958).
5. H. F. Ramstad and F. D. Richardson with Appendix by P. J. Bowles, *Trans. AIME* **221**, 1021 (1961).
6. G. L. Humphrey, S. S. Todd, J. P. Coughlin, and E. G. King, US Bureau of Mines, Bulletin No. 4888 (1952).
7. N. A. Toropov and V. P. Barzakovskii, "High Temperature Chemistry of Silicates and Other Oxide Systems," Special Report, Consultants Bureau, New York (1966).
8. K. Schwerdtfeger, *Trans. AIME* **236**, 1152 (1966).
9. M. S. Crowley, *Bull. Amer. Ceram. Soc.* **46**, 679 (1967); **49**, 527 (1970).
10. J. D. Hancock and J. H. Sharp, *J. Amer. Ceram. Soc.* **55**, 74 (1972).
11. W. A. Johnson and R. F. Mehl, *Trans. AIME* **135**, 416 (1939).
12. M. Avrami, *Chem. Phys.* **7**, 1103 (1939); **8**, 212 (1940); **9**, 177 (1941).
13. B. V. Erofe'ev, *C.R. Dokl. Acad. Sci. URSS* **52**, 511 (1946).